# Peptide adsorption on silica surfaces: Simulation and experimental insights

Mikhail Suyetin [a], Stefan Rauwolf [b], Sebastian Patrick Schwaminger [b,c,*], Chiara Turrina [b], Leonie Wittmann [b], Saientan Bag [a], Sonja Berensmeier [b,**], Wolfgang Wenzel [a,**]

[a] Institute of Nanotechnology, Karlsruhe Institute of Technology, Hermann-von-Helmholtz-Platz 1, 76344, Eggenstein-Leopoldshafen, Germany
[b] Bioseparation Engineering Group, School of Engineering and Design, Technical University of Munich, 85748, Garching, Germany
[c] Division of Medicinal Chemistry, Otto Loewi Research Center, Medical University of Graz, 8010, Graz, Austria

ARTICLE INFO

*Keywords:*
Rapid Simulation
Aminoacids
Adsorption
Implicit solvent
Implicit surface

ABSTRACT

The understanding of interactions between proteins with silica surface is crucial for a wide range of different applications: from medical devices, drug delivery and bioelectronics to biotechnology and downstream processing. We show the application of EISM (Effective Implicit Surface Model) for discovering the set of peptide interactions with silica surface. The EISM is employed for a high-speed computational screening of peptides to model the binding affinity of small peptides to silica surfaces. The simulations are complemented with experimental data of peptides with silica nanoparticles from microscale thermophoresis and from infrared spectroscopy. The experimental work shows excellent agreement with computational results and verifies the EISM model for the prediction of peptide-surface interactions. 57 peptides, with amino acids favorable for adsorption on Silica surface, are screened by EISM model for obtaining results, which are worth to be considered as a guidance for future experimental and theoretical works. This model can be used as a broad platform for multiple challenges at surfaces which can be applied for multiple surfaces and biomolecules beyond silica and peptides.

## 1. Introduction

The understanding of the nature of protein-surface interaction plays an important role for applications in medical implants, biotechnology, biosensors, and for biological/electronic interfaces, etc. An overwhelming amount of experimental and theoretical studies is focused on investigating the interaction between peptides, proteins, and inorganic surfaces [1–6], and, specifically, silica - relatively cheap and technologically convenient material for different biological applications [7–9]. The peptides - silica interactions are exhaustively studied in [10,11], and it is proved the leading role of Lys, Arg, and Ser amino acids for adsorption enhancing on silica surface [12].

Multiple techniques exist which focus on the characterization of biomolecule-surface interactions.

The most prominent characterization tools for the experimental analysis of biomolecule-surface interactions are the following: quartz crystal microbalance (QCM), surface plasmon resonance (SPR), isothermal titration calorimetry (ITC) and microscale thermophoresis (MST). QCM and SPR are based on the adsorption of biomolecules at flat surfaces, where the interaction can be measured as a change in the vibration frequency due to adsorption of molecules and the resulting gain in mass or as a phase shift due to a change in the surface plasmonic structure, respectively [13,14]. Even though restricted to flat surfaces, especially SPR is the standard method for the analysis of protein surface interactions [3]. A recently developed method for studying interactions in recent years is MST, first described in 2010 by Duhr and co-workers as a method to analyze interactions of proteins and small molecules in biological fluids [15]. MST is an optical method using thermophoresis, the directed motion of fluorescent labeled molecules induced by a temperature gradient, to measure the dissociation constant ($K_D$) of interactions [16–21]. MST offers many advantages compared to classical methods such as ITC, fluorescence polarization (FP), SPR, dynamic light scattering (DLS), and so on. MST allows for the in vitro analysis of particulate systems and is based on the size-dependent diffusion which allows to analyse binding event and therefore the affinity between two substances [15,22]. ITC is also suited for the characterization of suspensions and the adsorption processes at nanoparticle surfaces. The MST, originally designed for protein-ligand interactions (i.e. other proteins, small molecules, ions), is shown to be also applicable with gold nanoparticles [23].

* Corresponding author at: Bioseparation Engineering Group, School of Engineering and Design, Technical University of Munich, 85748, Garching, Germany.
** Corresponding authors.
*E-mail addresses:* sebastian.schwaminger@medunigraz.at (S.P. Schwaminger), S.Berensmeier@tum.de (S. Berensmeier), Wolfgang.Wenzel@kit.edu (W. Wenzel).

There are multiple further techniques which allow for biomolecule-surface characterization which are less efficient and use spectroscopic or calorimetric approaches [3]. All of these approaches have their advantages and disadvantages but allow for an affinity determination even though the affinities might slightly diverge for different approaches. Affinities between surfaces and proteins are usually in the nanomolar and micromolar range for specific binding.

Simulation approaches can give valuable insights from the phenomena studied to go beyond than just complementary calculations for supporting experimental work [24–26]. Classical Molecular Dynamics (MD) and Monte Carlo (MC) are widely used computational techniques for studying adsorption phenomena in details [27–29]. These approaches are employing mostly classical force fields (FF) for the simulations to study peptides sorption on surfaces [30–34].

The parameters of FF are obtained from highly precise ab initio simulations, experimental data, or machine learning calculations. In order to go further: to get the large conformation space of peptides and study much bigger systems with a smaller computational effort (less computational time) than all-atoms models, an implicit model for the surface and the solvent is applied. There are two advantages of this model: (1) – computational cost is significantly reduced thanks to decreasing the number of the degrees of freedom in the simulation to the internal degrees of freedom of the peptide and its center-of-mass coordinates; (2) – the model can use buffer and surfaces conditions.

In this work we show the application of EISM model within SIMONA simulation package for discovering the set of peptide interactions with silica surface, previously it is successfully done for gold surface [5]. In order to get experimental insights on the peptide-silica interaction the necessary experimental studies are performed by MST technique. The interactions of amino acids are parameterized with the surface studied employing the data from All atom MD calculations. The results obtained for peptide binding with silica surfaces are in excellent agreement with All atom MD results and, more importantly, with experimental data performed by MST technique. In the following we introduce an implicit solvent / implicit surface force field, the Effective Implicit Surface Model (EISM), for fast and efficient *in silico* evaluation of the binding affinity of peptides with inorganic surfaces. The EISM calculations shows exceptional speed in comparison to All atom MD.

**The novelty of this model** is to employ implicit solvent/implicit surface model, which is parameterized from the experimentally or computationally obtained values of affinity of amino acids and can be subsequently used to compute trends in the affinity of peptides to the same surface.

**The new insights** is the positively charged peptides bind to silica with a high affinity and the simulation is able to predict affinity and binding peptides to silica and ideally multiple surfaces. The experiment is a validation of the simulation. We see binding in both systems and therefore the simulation seems to work quite well.

## 2. Methods

### 2.1. Effective implicit surface model

SIMONA package is employed for EISM calculations using Monte Carlo approach. EISM is a part of SIMONA: http://int.kit.edu/nanosim/simona.

In the following we introduce an implicit solvent / implicit surface force field, The Effective Implicit Surface Model (EISM) consist of the following terms for application of implicit solvent and implicit surface force field:

$$E = E_{INT} + E_{SLIM} + \quad E_{SLJ} + E_{SASA} + E_{PIT} \tag{1}$$

$\boldsymbol{E_{INT}}$ – internal energy: Lennard-Jones, Coulomb and dihedral term are parametrized by standard force field available. In this investigation we have used the AMBER99IDLN force field [27–29].

$\boldsymbol{E_{SLIM}}$ – an implicit membrane model for the simulation of the electrostatic interactions between the peptide and the surface. SLIM based on a layered Generalized Born model.

A peptide has a dielectric constant $\epsilon_c = 1$, the surface is modeled as a single dielectric slab from silica has a dielectric constant $\epsilon_h = 3.9$, and the solvent has $\epsilon_w = 80$.

$\boldsymbol{E_{SLJ}}$ is the Lennard Jones interactions between the amino acid and silica surface.

$$E_{\mathrm{SLJ}} = 8\sum_i \sqrt{\epsilon_i \epsilon_S} * \left( \left( \frac{0.5 \quad (\sigma_i + \sigma_S)}{z_i \quad z_S \quad \sigma_S} \right)^9 \quad \left( \frac{0.5 \quad (\sigma_i + \sigma_S)}{z_i \quad z_S \quad \sigma_S} \right)^3 \right) \tag{2}$$

$\sigma_i$ and $\epsilon_i$ are the Lennard-Jones parameters of the peptide's atoms; $\sigma_S = 3.5\,\AA$ and $\epsilon_S =$ 0.1kcal/mol are parameters of the surface. This term keeps a peptide from penetrating into the surface region. $Z_S$- z-position of the surface is defined by the parameter.

$\boldsymbol{E_{SASA}}$ - is to describe the interaction of a peptide and surface taking into account solvent accessible surface (SASA) of the peptide and a residue-specific surface tension - $\gamma_{aa}$ (units kJ/mol/Å$^2$):

$$E_{SASA} = \sum_i \gamma_{aa} f(z_i \quad z_S) A_i + \gamma_w \sum_i A_i \tag{3}$$

All specific interactions of the peptide with the surface are parameterized by a short-range contact potential represented in the third term in Eq. 1 (solvent accessible surface area) is used to model the interactions of individual amino acids with the surface that are not accounted for by the previously described interactions. $\gamma_{aa}$ determines the maximum strength of the interaction. The strength of the interaction is a function of the distance by the switching function $f(z_i \quad z_S)$. $\gamma_{aa}$ is defined by fitting to the experimental/theoretical data for a specific surface and conditions.

$\boldsymbol{E_{PIT}}$ – is to keep peptide in a simulation box.

### 2.2. Classical MD simulations

#### 2.2.1. US using all-atom molecular dynamic (MD) simulations

From the pH dependent atomistic silica surface model database [35], we chose Q3 silica surface model having 4.7 silanol groups per nm$^2$ of the surface of which 14 % are deprotonated corresponding to a pH of 7.4. The atomistic model of the amino acids (AA) were build using TLEAP module of AMBERTOOLS package [2]. To start with, we prepared a simulation box with the silica surface in one end and AA in the middle as shown in Fig. 1. The full system was then solvated in TIP3P water and sufficient numbers of $Na^+$ and $Cl^-$ counter ions were added to achieve overall charge neutrality of the system. The force field (FF) parameters involving silica surface atoms were taken from silica surface model database of Emami et al. [35], while the rest of the FF parameters were collected from AMBER99SB-ILDN FF [36]. We first energy minimized the full system using steepest descent algorithm. With the energy minimized system, we further performed MD simulation in NVT ensemble to equilibrate the system. The silica surface were kept fixed during the entire simulation run and periodic boundary condition was applied in all three directions. We used Nose-Hoover thermostat to maintain the system temperature at 300 K. A series of short NVT simulations with varying z dimensions (perpendicular to the surface) of the box were performed thereafter to achieve the correct density of the water in the bulk. The system with correct water density was further used for the subsequent MD runs. The AA was then pulled towards the silica surface and was allowed to be adsorbed (to the silica). We equilibrated the system again when the AA was adsorbed to the silica. To prepare the system for the US run, the AA was pulled away from the silica surface and system configurations were saved at a distance (between the center of mass of AA and the silica surface) interval of 0.1 Å. Therefore, the reaction coordinate (see Fig. 1) for the US run was the distance between silica surface and the center of mass of AA. The US simulations were performed with these system configurations where the strength of the umbrella potential was fixed at 1000 kJ mol nm $^2$. We

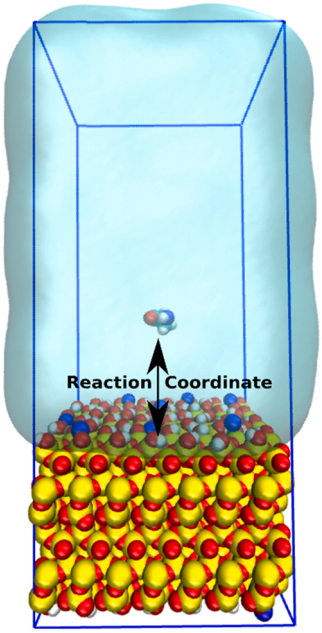


**Fig. 1.** Snapshot of the initial system prepared for MD simulation with silica surface in one end and AA in the middle of the simulation box. The surrounding water medium is not shown in full atomistic details but as translucent surfaces for clarity. The reaction coordinate for the US run is highlighted by a two-way arrow.

first equilibrate each US windows for 4 ns and then from another 10 ns run, we save the data for the further analysis to generate the histograms of the reaction coordinate. Weighted Histogram Analysis Method (WHAM) was used to generate the potential of mean force (PMF) curve from the histograms. All the MD simulations were performed in GROMACS software package.

## 3. Results

Fluorescent silica particles is synthesized and characterize according to their chemical composition and their size and shape. The attenuated total reflection infrared (ATR-IR) spectrum of the synthesized a dried particles shows the presence of Si-O-Si vibrations corresponding to the peak at around 1065 cm $^{1}$ and other peaks corresponding to Si-O vibrations at 947 and 796 cm $^{1}$ (Fig. 2a) [37,38]. Furthermore, terminal O-H stretching vibrations are visible between 3200 and 3500 cm $^{1}$. [37] On the other hand, we are not able to observe a significant peak corresponding to FITC vibrations which indicates a complete coating. [39] The hydrodynamic diameter of the synthesized particles is around 50 nm which is in good agreement with literature and indicates a great stabilization of the nanoparticles in aqueous media (Fig. 2b) [39]. The hydrodynamic diameter is only slightly larger than the diameter obtained from analyzing TEM images of the synthesized particles. The stability of the particles is due to a complete coating of silica and electrostatic repulsion forces, which can be shown by the negative zeta potenial of around 44 mV which is also in good agreement with the literature for silica coated fluorescent nanoparticles [40]. Thus, the particles are colloidally stable nanoparticles which can be used as fluorescent marker in microscale thermophoreses to determine the interaction between silica surfaces and biomolecules. The electron

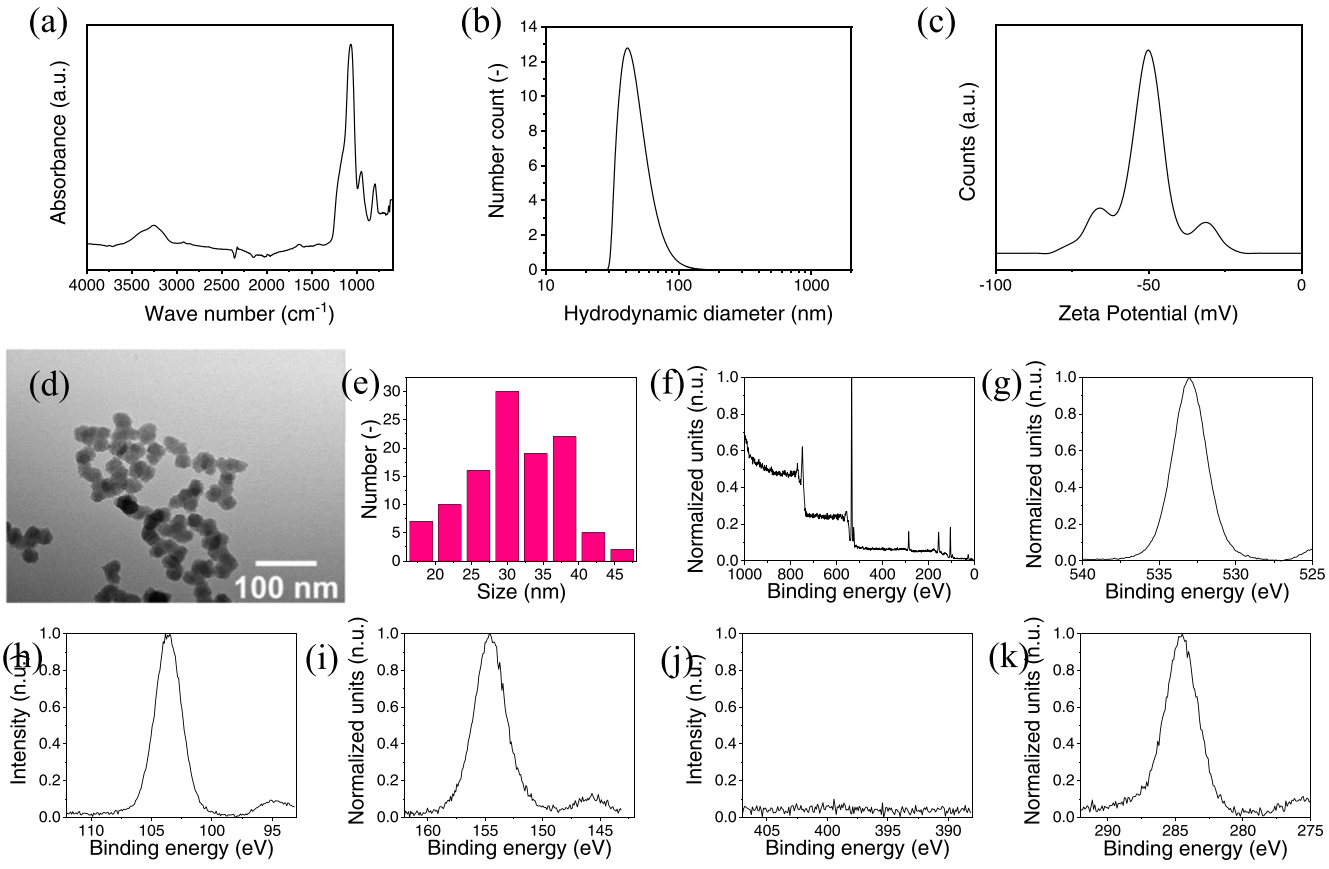


**Fig. 2.** ATR-IR spectrum of fluorescent silica particles (a). Hydrodynamic diameter is from dynamic light scattering of fluorescent silica particles (b). Zeta potential of fluorescent silica nanoparticles (0.5 g $L^{-1}$) at pH 7 in deionized water (c). TEM image of fluorescent silica particles (d) and histogram of TEM (e). X-ray photoelectron spectrum of fluorescent silica particles. Survey (f), O1s region (g), Si2p region (), Si2s region (i), N1s region (j) and C1s region (k).

microscopy images indicate particle sizes ranging from 15 to 50 nm with a maximum at 30–35 nm (Fig. 2d and e). The surface composition of the nanomaterials as obtained from XPS analysis mainly indicates silicon and oxygen being present, while no traces of nitrogen can be observed (Fig. 2f-j). The peak corresponding adventitious carbon does not indicate fluorescamine isothiocyanate (FITC) and sp2 hybridized carbon but represents a typical shape which is known for other bare nanomaterials in literature (Fig. 2k). The deconvolution of the O1s spectrum indicates the presence of oxygen bound to silicon as well as hydrates [41]. The shape of both silicon spectra are typical for silica and definitely verify the presence of silica on the surface of the nanoparticles (Fig. 2h and i) [41].

The EISM residue-specific surface tension parameters $\gamma_{aa}$ (where *aa* = 20 amino acids) for Silica surface are identified by Monte-Carlo simulations (SIMONA) in combination with US (PLUMED).

It is suggested to employ in EISM simulations $\gamma_i$ is decreased by 10 %. [5] The values of $\gamma_i$ are shown in the Table 1.

The peptides are created in TLEAP module of AMBERTOOLS package for EISM calculations. The peptides are mostly uncapped. Other peptides are capped at N- and C-terminal with Acetyl and N-methyl group respectively. Peptides are relaxed in the presence of the explicitly treated water without any surfaces employing classical molecular dynamics simulation with the AMBER99SB-ILDN force field and SPC water model for 200 ns using the GROMACS simulation package. The Nosé –Hoover thermostat keep temperature at 300 K and pressure at 1 atm with the Parinello–Rahman barostat. Monte Carlo simulations with EISM model is performed with SIMONA package to investigate the interactions of peptides with Silica surface at 300 K using PLUMED – US protocol [42–44]. The free energy of binding curves is averaged through twenty independent simulations for every single peptide sequence in order to decrease the numerical error. The PMF (Potential of Mean Force) is calculated using WHAM. The details of ESIM model are shown in SI.

The EISM model calculations are used for the big list of peptides, employing $\gamma_{aa}$ parameterization on from All-atom MD simulations obtained previously. In case of lasioglossin (LL) and WRHRHRHRH peptide [$(RH)_4$] binding affinities (ΔG) to the silica surface are experimentally measured by microscale thermophoresis (MST) technique, and show excellent agreement between simulation data and experimental values. The difference in Gibbs free energy between the bound and the unbound state with silica surface is the binding affinity of a peptide.

Simulation are performed with EISM model is focused on isolated peptide, not a monolayer. The free energy of adsorption obtained by EISM model can be rescaled from a single peptide value to a monolayer of peptides at a finite concentration according to approach [45]. The excellent agreement is found between ΔG from EISM model and further rescaled and ΔG from MST experiment. In case of LL: $\Delta G_{EISM}$(LL) = 43.1 kJ/mol, $\Delta G_{RESCALED}$(LL) = 23.3 kJ/mol, $\Delta G_{MST}$(LL) = 23.7 kJ/mol. In case of RH4: $\Delta G_{EISM}$(RH4) = 50.7 kJ/mol, $\Delta G_{RESCALED}$(RH4) = 27.4 kJ/mol, $\Delta G_{MST}$(RH4) = 29.1 kJ/mol. (Table 2).

**Table 1**
Adsorption free energies (kJ/mol) at the Silica interface for all 20 amino acids and $\gamma_{aa}$ from EISM.

| Amino acids | ΔG kJ/mol | EISM $\gamma_i$ | Amino acids | ΔG kJ/mol | EISM $\gamma_i$ |
|---|---|---|---|---|---|
| **ALA (A)** | -15.75 | -1.44 | **LEU (L)** | -12.73 | -0.72 |
| **ARG (R)** | -23.52 | -1.05 | **LYS (K)** | -23.95 | -0.99 |
| **ASN (N)** | -16.58 | -0.99 | **MET (M)** | -17.59 | -1.35 |
| **ASP (D)** | -6.20 | -0.23 | **PHE (F)** | -20.26 | -1.44 |
| **CYS (C)** | -14.17 | -0.54 | **PRO (P)** | -16.68 | -1.35 |
| **GLN (Q)** | -19.05 | -1.08 | **SER (S)** | -13.06 | -0.63 |
| **GLU (E)** | -13.25 | -0.63 | **THR (T)** | -12.69 | -0.72 |
| **GLY (G)** | -15.22 | -1.53 | **TRP (W)** | -18.31 | -1.08 |
| **HIS (H)** | -20.49 | -1.44 | **TYR (Y)** | -23.65 | -1.53 |
| **ILE (I)** | -13.60 | -0.81 | **VAL (V)** | -15.21 | -1.35 |

**Table 2**
EISM results of adsorption free energies (kJ/mol) at the silica interface for a list of peptides, and results of available experimental data for monolayer and conversion for values for one peptide.

| Name of peptide | Sequence | EISM, ΔG (kj/mol) One peptide | Rescaled for monolayer ΔG (kj/mol) | MST experiments, ΔG, (kj/mol) Monolayer |
|---|---|---|---|---|
| **LL** | VNWKKILGKIIKVVK | -43.1 | -23.3 | -23.7 |
| **RH4** | WRHRHRHRH | -50.7 | -27.4 | -29.1 |

Microscale thermophoresis of peptides as ligands for fluorescent silica nanoparticles yields high affinities of 12.47 μM and 16.01 μM for $(RH)_4$ and lasioglossin in TRIS buffer, respectively. These affinities are in very good agreement with other silica-binding peptides and with the simulation data. [46] The sigmoidally shaped isotherm indicates a Langmuir-like binding behavior for both peptides on silica in the logarithmically scaled Fig. 3 [16,22,47]. The inflection points indicating the affinity or dissociation constant can be very well observed within the investigated concentration range. Furthermore, onset and maximum bound fraction can be observed in both thermophoresis plots which allow a fit with high significance and therefore allow a good interpretation of the data. Hence, both proteins not only bind to silica but indeed demonstrate a high affinity. The measured equilibrium constants ($K_D$ = 16.01 μM; 12.47 μM) yield adsorption free energies ΔG of 27.991 kJ and 27.371 kJ for $(RH)_4$ and lasioglossin in TRIS buffer, respectively. These results are very similar to the values of free energies from EISM and thus represent a very well suited validation of the model and its qualitative prediction.

Attenuated total reflection infrared spectroscopy (ATR-IR) indicates a distinct binding and surface complexation of silica nanoparticles by both investigated peptide ligands ($(RH)_4$ and lasioglossin) as shown in Fig. 4. The naked silica spectrum demonstrates Si-O-Si stretch vibrations around 1080 $cm^{-1}$ and Si-O vibrations at 950 $cm^{-1}$ [37,39]. Furthermore, small contributions of surface-bound water can be observed at 3000–3600 $cm^{-1}$ in form of a O-H stretching vibration and an O-H bending vibration at 1600 $cm^{-1}$ [37]. The broad bands at 1650 $cm^{-1}$ corresponding to amine and amides from both peptides indicate an interaction between the silica surface and the peptides [48]. Both spectra are conducted after washing the silica particles twice which indicates a specific and long-lasting binding of both peptides. The more pronounced C-H vibrations at 2800–3000 $cm^{-1}$ and the amide bands at 1650 $cm^{-1}$ and 1500 $cm^{-1}$ for $(RH)_4$ might indicate a stronger binding to the silica surface than lasioglossin since lasioglossin contains more amines in its native structure.

The Simona simulation package has a greatly improved computational speed (the comparison with classical MD is shown later), which gives an opportunity to perform a screening, and more importantly, to make an analysis from the data obtained. CotB1p T3 is chosen as a starting point for revealing the influence of amino acids in adsorption free energy. Amino acids in CotB1p T3 are replaced by ALA, as it shown in Table 3, where the name of peptide, sequence are presented along with the values of free energy of adsorption calculated for the each of peptide (SB7 M1–7). In order to estimate the impact on adsorption by each amino acid in CotB1p T3, the difference of adsorption free energy values of CotB1p T3 and SB7 M1–7 is calculated and presented in Table 3 as Δ. Considering two sequences RQSSRGR and AQSSRGR, it is seen that ΔG of later is a bit lower (Δ = 1.7 kj/mol), that can be explained that adsorption free energy of ARG is lower than in case of ALA, (please, see Table 1). The next pair is RQSSRGR and RASSRGR: the difference between two values of adsorption free energy is small ( 0.9 kj/mol), that is coming from not very large difference in ΔG of ALA and GLN (Table 1). The pair RQSSRGR and RQASRGR shows opposite difference, than in previous cases: Δ = 1.4 kj/mol, which has a solid ground – ΔG of ALA is bigger than ΔG of SER (see Table 1). The positive

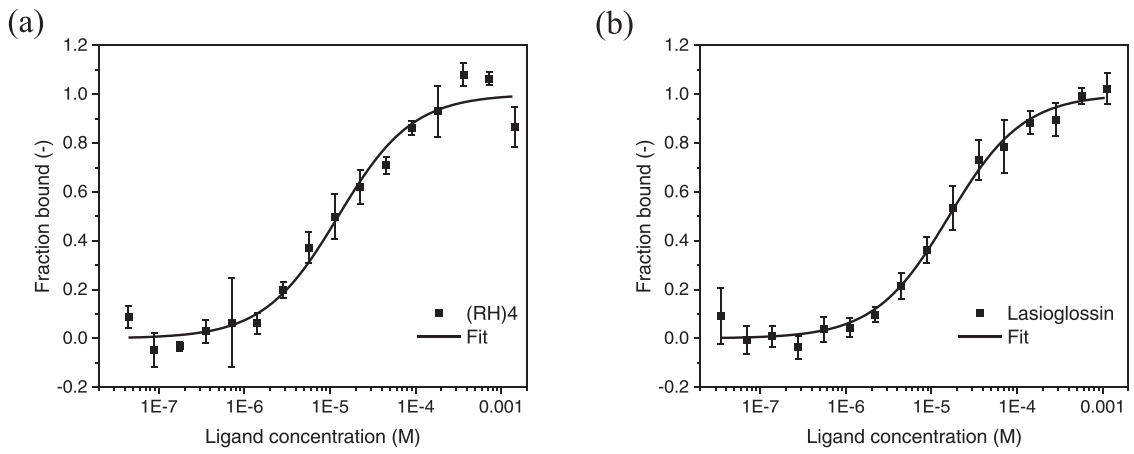


**Fig. 3.** Microscale thermophoresis plots for $(RH)_4$ (a) and lasioglossin (b) on nanoscale fluorescent silica particles. The experiments are performed with TRIS buffer at pH 7.4. Sixteen different ligand (peptide) concentrations ranging from around 2 nm to 1 mM are investigated. All experiments are conducted in triplicates.

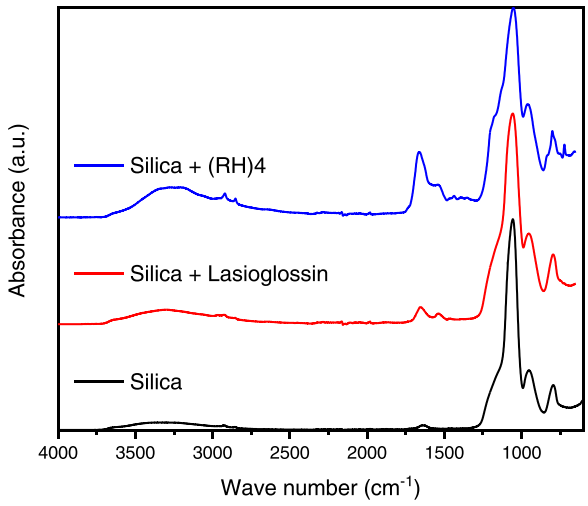


**Fig. 4.** ATR-IR spectra of bare silica as well as lasiglossin and $(RH)_4$ bound to silica in water at pH7 and washed two times with deionized water.

**Table 3**
Analysis of the amino acid influence on adsorption free energy change of CotB1p T3 peptide.

| Name of peptide | Sequence | | | | | | | ΔG (kj/mol) | Δ (kj/mol) |
|---|---|---|---|---|---|---|---|---|---|
| SB7 M1 | **A** | Q | S | S | R | G | R | -28.2 | -1.7 |
| SB7 M2 | R | **A** | S | S | R | G | R | -29.0 | -0.9 |
| SB7 M3 | R | Q | **A** | S | R | G | R | -31.3 | 1.4 |
| SB7 M4 | R | Q | S | **A** | R | G | R | -31.1 | 1.2 |
| SB7 M5 | R | Q | S | S | **A** | G | R | -27.2 | -2.7 |
| SB7 M6 | R | Q | S | S | R | **A** | R | -30.1 | 0.2 |
| SB7 M7 | R | Q | S | S | R | G | **A** | -28.4 | -1.5 |
| CotB1p T3 | R | Q | S | S | R | G | R | -29.9 | 0.0 |

Δ (1.2 kj/mol) is observed for the pair RQSSRGR and RQSARGR like in a previous case. The negative energy difference (Δ = 2.7 kj/mol) is observed for the pair RQSSRGR and RQSSAGR, which is consistent with the fact, that adsorption free energy for ARG is bigger than for ALA. The positive Δ (0.2 kj/mol), but close to zero is observed for the pair RQSSRGR and RQSSRAR, which is in a good agreement with fact that that adsorption free energy for GLY is very close to ALA. The last pair of sequences considered is RQSSRGA and RQSSRGR with the negative energy difference (Δ = 1.5 kj/mol). It should be noted that this value is close to Δ = 1.7 kj/mol of pair RQSSRGR and AQSSRGR, where ALA is at the one end of peptide and in case of RQSSRGA it is at the other end of peptide. In case of RQSSAGR, where ALA is in the middle of peptide the different values is observed: Δ = 2.7 kj/mol.

Also, simulations are performed for M P1–7 peptides, where M P1 is chosen as a starting point for revealing the influence of amino acids in adsorption free energy. Consistently, amino acids in M P1 are replaced by ALA (Table 4), where the name of peptide sequence are presented with the values of adsorption free energy (M P1–7). In order to estimate the impact on adsorption by each amino acid in M P1–7, the difference of adsorption free energy values of M P1–7 and M P2–7 is calculated and presented in Table 4 as Δ.

The first pair of sequences is QPASSRY and APASSRY, where Δ = 0.2 kj/mol, because GLN shows bigger free energy of adsorption (Table 1). Next pair is QPASSRY and QAASSRY where Δ = 1.5 kj/mol, taking into account that PRO exhibits greater free energy than ALA. Completely different picture is observed with positive Δ = 0.2 kj/mol for the pair QPASSRY and QPAASRY, because SER shows lower free energy of adsorption than ALA. Larger positive Δ = 2.2 kj/mol is observed for the pair QPASSRY and QPASARY. For the last two pairs QPASSRY - QPASSAY, and QPASSRY – QPASSA negative values of Δ are observed ( 1.2 kj/mol and 0.6 kj/mol, respectively), due to the larger free energy of adsorption of ARG and TYR, respectively.

Additionally, the simulation are performed for sorption investigation of LKalpha14 capped with an acetyl group and carboxyl amide group. The free energy of adsorption equals to 62.9 kj/mol, which is in a good agreement with available data from All-atom MD simulations: 58.2 kj/mol. [49].

Simona simulation package needs only minutes for performing necessary simulations of amino acid / peptide sorption on Silica surface, in comparison to classical MD. There are two remarkable comparisons in Table 5: classical MD needs hundreds of hours to perform simulation of amino acid ALA or peptide AAA adsorption of Silica Surface. Simona

**Table 4**
Analysis of the amino acid influence on adsorption free energy change of M P1 peptide.

| Name of peptide | Sequence | | | | | | | ΔG (kj/mol) | Δ (kj/mol) |
|---|---|---|---|---|---|---|---|---|---|
| M P2 | **A** | P | A | S | S | R | Y | -28.8 | -0.2 |
| M P3 | Q | **A** | A | S | S | R | Y | -27.5 | -1.5 |
| M P4 | Q | P | A | **A** | S | R | Y | -29.2 | 0.2 |
| M P5 | Q | P | A | S | **A** | R | Y | -31.2 | 2.2 |
| M P6 | Q | P | A | S | S | **A** | Y | -27.8 | -1.2 |
| M P7 | Q | P | A | S | S | R | **A** | -28.4 | -0.6 |
| M P1 | Q | P | A | S | S | R | Y | -29.0 | 0.0 |

**Table 5**
The comparison of simulation time and adsorption free energy between MD (Gromacs) and SIMONA for A and AAA.

| System studied | MD + US | ΔG, (kj/mol) | EISM + US | ΔG, (kj/mol) |
|---|---|---|---|---|
| **A** | ~236 h | -15.75 | ~ 15 min | -15.75 |
| **AAA** | ~250 h | -22.01 | ~ 16 min | -23.71 |

needs only 15 min for ALA adsorption simulation employing EISM approach, and 16 min in case of peptide AAA. The greatly improved computational speed gives an opportunity for high-throughput computational screening of peptides with revealing hidden dependencies and trends. The attempt of performing computational screening is performed in this paper: 57 peptides are simulated. The full list of peptides studied is shown in Table S1.

Different peptides (totally 57) with a content of amino acids, which are favorable for adsorption on silica surface, are screened within this work for revealing the free energy of adsorption. These data can be employed as a reference point for further research work.

In this paper, we have so far established the EISM model as an efficient tool to calculate adsorption free energy of peptides with unprecedented computational efficiency. However, having similar free energy of adsorption do not guarantee similar adsorption behavior. To look more into it we also compared the whole free energy curves (which captures the binding behavior) for an amino acid (A) and a peptide (AAA) obtained from MD and EISM.

As it is evident from Figs. 4–5 that the nature of the free energy curve are very similar in both the cases (MD and EISM). We would like to emphasize that EISM is a coarse-grained model which was developed far fast calculation of peptide free energy and therefore we do not except more quantitative agreement in capturing the adsorption behavior with the all-atom MD calculation.(Fig. 6).

## 4. Conclusions

The application of EISM model for peptide/silica surface interactions study is presented. The necessary residue-specific surface tension parameters for the EISM model are obtained from All-atom MD simulations of amino acids interactions with silica surface. Delightfully, the simulations show an excellent agreement with experimental results obtained via MST technique utilizing fluorescent silica nanoparticles. Also, EISM results shows nice agreement with All-atoms.

The computational speed comparison shows that Simona employing EISM model needs only minutes to perform calculation, but classical MD approach needs hundreds of hours for the same work. The combination of implicit solvent and implicit surface in EISM model gives a tremendously exciting opportunity for performing high-throughput screening of peptides with revealing hidden dependencies and trends via machine learning approaches in the future work.

The two successful attempts of computational screening take place within this work: CotB1p T3 and the set of sequences SB7 M1–7; also, MP1 and set of sequences MP2–7. The influence of different amino acids on adsorption free energy is revealed. Totally, 57 peptides of different length are simulated for adsorption on Silica surface. The results of free energy of adsorption obtained for these peptides are worth to be employed as a guidance for future experimental and theoretical works.

## CRediT authorship contribution statement

**Mikhail Suyetin**: Investigation, Software, Validation, Visualization, Conceptualization, Formal analysis, Writing – original draft, Writing – review & editing. **Stefan Rauwolf**: Investigation, Writing – original draft. **Sebastian Patrick Schwaminger**: Investigation, Supervision, Conceptualization, Writing – original draft, Writing – review & editing. **Chiara Turrina**: Investigation. **Leonie Wittmann**: Investigation. **Saientan Bag**: Investigation, Writing – review & editing. **Sonja Berensmeier**: Conceptualization, Methodology. **Wolfgang Wenzel**: Supervision, Conceptualization, Methodology, Software, Writing – review & editing.

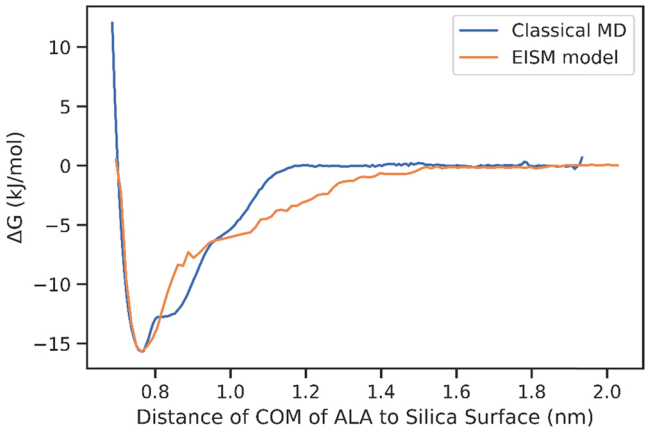


**Fig. 5.** The comparison of free energy of adsorption of ALA obtained by EISM and MD.

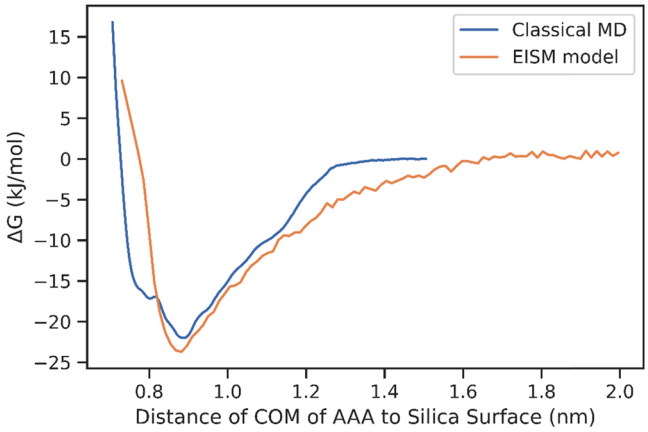


**Fig. 6.** The comparison of free energy of adsorption of AAA obtained by EISM and MD.

## Declaration of Competing Interest

The authors declare that they have no known competing financial interests or personal relationships that could have appeared to influence the work reported in this paper.

## Data availability

Data will be made available on request.

## Acknowledgments

For financial support, the authors would like to acknowledge the funded by the Federal Ministry of Education and Research (Grant No. 031A173B and 031A095C), support by TUM International Graduate School of Science and Engineering (IGSSE) as well as of GRK2450, "Tailored scale bridging approaches to computational nanoscience" and Marie Skłodowska Curie actions of the European Commission (project 887412, NERS). Furthermore, the undergraduate students Florian Schnell and Aylin Yilmaz are acknowledged for their help with particle synthesis.

*Author contributions*

M.S., and S.B. performed calculations. S.P.S, and So.B. designed the experimental approach. S.R., S.P.S, and C.T. characterized the samples. S.R., S.P.S., and C.T. performed microscale thermophoresis and infrared spectroscopy. C.T., and L.W. carried out TEM experiments. M.S., and W. W. software development and conceived the theoretical part of the project. M.S., S.B. S.R, S.P.S, So.B., and W.W. wrote the paper. All authors discussed the results and implications and commented on the manuscript.

## Appendix A. Supporting information

Supplementary data associated with this article can be found in the online version at doi:10.1016/j.colsurfb.2022.112759.

## References


[1] S. Maity, D. Zanuy, Y. Razvag, P. Das, C. Alemán, M. Reches, Elucidating the mechanism of interaction between peptides and inorganic surfaces, Phys. Chem. Chem. Phys. 17 (2015) 15305–15315.

[2] A. Vallee, V. Humblot, C.-M. Pradier, Peptide interactions with metal and oxide surfaces, Acc. Chem. Res. 43 (2010) 1297–1306.

[3] S. Schwaminger, S.A. Blank-Shim, M. Borkowska-Panek, P. Anand, P. Fraga-García, K. Fink, W. Wenzel, S. Berensmeier, Experimental characterization and simulation of amino acid and peptide interactions with inorganic materials, Eng. Life Sci. 18 (2018) 84–100.

[4] Z. Tang, J.P. Palafox-Hernandez, W.-C. Law, Z.E. Hughes, M.T. Swihart, P. N. Prasad, M.R. Knecht, T.R. Walsh, Biomolecular recognition principles for bionanocombinatorics: an integrated approach to elucidate enthalpic and entropic factors, ACS Nano 7 (2013) 9632–9646.

[5] M. Suyetin, S. Bag, P. Anand, M. Borkowska-Panek, F. Gußmann, M. Brieg, K. Fink, W. Wenzel, Modelling peptide adsorption energies on gold surfaces with an effective implicit solvent and surface model, J. Colloid Interface Sci. 605 (2022) 493–499.

[6] Z.E. Hughes, M.A. Nguyen, J. Wang, Y. Liu, M.T. Swihart, M. Poloczek, P.I. Frazier, M.R. Knecht, T.R. Walsh, Tuning materials-binding peptide sequences toward gold- and silver-binding selectivity with bayesian optimization, ACS Nano 15 (2021) 18260–18269.

[7] S.V. Patwardhan, F.S. Emami, R.J. Berry, S.E. Jones, R.R. Naik, O. Deschaume, H. Heinz, C.C. Perry, Chemistry of aqueous silica nanoparticle surfaces and the mechanism of selective peptide adsorption, J. Am. Chem. Soc. 134 (2012) 6244–6256.

[8] S. Rauwolf, S. Bag, R. Rouqueiro, S.P. Schwaminger, A.C. Dias-Cabral, S. Berensmeier, W. Wenzel, Insights on alanine and arginine binding to silica with atomic resolution, J. Phys. Chem. Lett. 12 (2021) 9384–9390.

[9] A. Sola-Rabada, M. Michaelis, D.J. Oliver, M.J. Roe, L. Colombi Ciacchi, H. Heinz, C.C. Perry, Interactions at the silica–peptide interface: influence of the extent of functionalization on the conformational ensemble, Langmuir 34 (2018) 8255–8263.

[10] P. Roach, D. Farrar, C.C. Perry, Surface tailoring for controlled protein adsorption: effect of topography at the nanometer scale and chemistry, J. Am. Chem. Soc. 128 (2006) 3939–3945.

[11] V. Puddu, C.C. Perry, Interactions at the silica–peptide interface: the influence of particle size and surface functionality, Langmuir 30 (2014) 227–233.

[12] E.L. Buckle, A. Roehrich, B. Vandermoon, G.P. Drobny, Comparative study of secondary structure and interactions of the R5 peptide in silicon oxide and titanium oxide coprecipitates using solid-state NMR spectroscopy, Langmuir 33 (2017) 10517–10524.

[13] I. Jelesarov, H.R. Bosshard, Isothermal titration calorimetry and differential scanning calorimetry as complementary tools to investigate the energetics of biomolecular recognition, J. Mol. Recognit. 12 (1999) 3–18.

[14] P. Taladriz-Blanco, N.J. Buurma, L. Rodríguez-Lorenzo, J. Pérez-Juste, L.M. Liz-Marzán, P. Hervés, Reversible assembly of metal nanoparticles induced by penicillamine. Dynamic formation of SERS hot spots, J. Mater. Chem. 21 (2011) 16880–16887.

[15] C.J. Wienken, P. Baaske, U. Rothbauer, D. Braun, S. Duhr, Protein-binding assays in biological liquids using microscale thermophoresis, Nat. Commun. 1 (2010) 100.

[16] M. Jerabek-Willemsen, T. André, R. Wanner, H.M. Roth, S. Duhr, P. Baaske, D. Breitsprecher, MicroScale thermophoresis: interaction analysis and beyond, J. Mol. Struct. 1077 (2014) 101–113.

[17] M. Jerabek-Willemsen, C.J. Wienken, D. Braun, P. Baaske, S. Duhr, Molecular interaction studies using microscale thermophoresis, ASSAY Drug Dev. Technol. 9 (2011) 342–353.

[18] S.A.I. Seidel, P.M. Dijkman, W.A. Lea, G. van den Bogaart, M. Jerabek-Willemsen, A. Lazic, J.S. Joseph, P. Srinivasan, P. Baaske, A. Simeonov, I. Katritch, F.A. Melo, J.E. Ladbury, G. Schreiber, A. Watts, D. Braun, S. Duhr, Microscale thermophoresis quantifies biomolecular interactions under previously challenging conditions, Methods 59 (2013) 301–315.

[19] S.A.I. Seidel, C.J. Wienken, S. Geissler, M. Jerabek-Willemsen, S. Duhr, A. Reiter, D. Trauner, D. Braun, P. Baaske, Label-free microscale thermophoresis discriminates sites and affinity of protein–ligand binding, Angew. Chem. Int. Ed. 51 (2012) 10656–10659.

[20] Y. Mao, L. Yu, R. Yang, L.-b Qu, P. d B. Harrington, A novel method for the study of molecular interaction by using microscale thermophoresis, Talanta 132 (2015) 894–901.

[21] N. Pantidos, L. Horsfall, Understanding the role of SilE in the production of metal nanoparticles by Morganella psychrotolerans using microscale thermophoresis, N. Biotechnol. 55 (2020) 1–4.

[22] M. Jerabek-Willemsen, C.J. Wienken, D. Braun, P. Baaske, S. Duhr, Molecular interaction studies using microscale thermophoresis, ASSAY Drug Dev. Technol . 9 (2011) 342–353.

[23] G. Wang, W. Wang, E. Shangguan, S. Gao, Y. Liu, Effects of gold nanoparticle morphologies on interactions with proteins, Mater. Sci. Eng. C 111 (2020), 110830.

[24] J.P. Ulmschneider, M.B. Ulmschneider, Molecular dynamics simulations are redefining our view of peptides interacting with biological membranes, Acc. Chem. Res. 51 (2018) 1106–1116.

[25] T.R. Walsh, Pathways to structure–property relationships of peptide–materials interfaces: challenges in predicting molecular structures, Acc. Chem. Res. 50 (2017) 1617–1624.

[26] L. Saiz, M.L. Klein, Computer simulation studies of model biological membranes, Acc. Chem. Res. 35 (2002) 482–489.

[27] M. Penaloza-Amion, E. Sedghamiz, M. Kozlowska, C. Degitz, C. Possel, W. Wenzel, Monte-Carlo simulations of soft matter using SIMONA: a review of recent applications, Front. Phys. 9 (2021).

[28] N. Heilmann, M. Wolf, M. Kozlowska, E. Sedghamiz, J. Setzler, M. Brieg, W. Wenzel, Sampling of the conformational landscape of small proteins with Monte Carlo methods, Sci. Rep. 10 (2020) 18211.

[29] M. Brieg, J. Setzler, S. Albert, W. Wenzel, Generalized born implicit solvent models for small molecule hydration free energies, Phys. Chem. Chem. Phys. 19 (2017) 1677–1685.

[30] M. Ozboyaci, D.B. Kokh, S. Corni, R.C. Wade, Modeling and simulation of protein–surface interactions: achievements and challenges, Q. Rev. Biophys. 49 (2016).

[31] F. Iori, R. Di Felice, E. Molinari, S. Corni, GolP: An atomistic force-field to describe the interaction of proteins with Au(111) surfaces in water, J. Comput. Chem. 30 (2009) 1465–1476.

[32] F. Iori, S. Corni, Including image charge effects in the molecular dynamics simulations of molecules on metal surfaces, J. Comput. Chem. 29 (2008) 1656–1666.

[33] J.A. Yancey, N.A. Vellore, G. Collier, S.J. Stuart, R.A. Latour, Development of molecular simulation methods to accurately represent protein-surface interactions: the effect of pressure and its determination for a system with constrained atoms, Biointerphases 5 (2010) 85–95.

[34] N.A. Vellore, J.A. Yancey, G. Collier, R.A. Latour, S.J. Stuart, Assessment of the transferability of a protein force field for the simulation of peptide-surface interactions, Langmuir 26 (2010) 7396–7404.

[35] F.S. Emami, V. Puddu, R.J. Berry, V. Varshney, S.V. Patwardhan, C.C. Perry, H. Heinz, Force field and a surface model database for silica to simulate interfacial properties in atomic resolution, Chem. Mater. 26 (2014) 2647–2658.

[36] M. Zgarbová, J. Šponer, M. Otyepka, T.E. Cheatham, R. Galindo-Murillo, P. Jurečka, Refinement of the sugar–phosphate backbone torsion beta for AMBER force fields improves the description of Z- and B-DNA, J. Chem. Theory Comput. 11 (2015) 5723–5736.

[37] P. Innocenzi, Infrared spectroscopy of sol–gel derived silica-based films: a spectra-microstructure overview, J. Non-Cryst. Solids 316 (2003) 309–319.

[38] H.-C. Roth, S.P. Schwaminger, F. Peng, S. Berensmeier, Immobilization of cellulase on magnetic nanocarriers, ChemistryOpen 5 (2016) 183–187.

[39] L. Cursi, S. Vercellino, M.M. McCafferty, E. Sheridan, V. Petseva, L. Adumeau, K. A. Dawson, Multifunctional superparamagnetic nanoparticles with a fluorescent silica shell for the in vitro study of bio-nano interactions at the subcellular scale, Nanoscale 13 (2021) 16324–16338.

[40] E. Mahon, D.R. Hristov, K.A. Dawson, Stabilising fluorescent silica nanoparticles against dissolution effects for biological studies, Chem. Commun. 48 (2012) 7970–7972.

[41] I. Tunc, S. Suzer, M.A. Correa-Duarte, L.M. Liz-Marzán, XPS characterization of Au (Core)/SiO2 (Shell) nanoparticles, J. Phys. Chem. B 109 (2005) 7597–7600.

[42] M. Bonomi, G. Bussi, C. Camilloni, G.A. Tribello, P. Banáš, A. Barducci, M. Bernetti, P.G. Bolhuis, S. Bottaro, D. Branduardi, R. Capelli, P. Carloni, M. Ceriotti, A. Cesari, H. Chen, W. Chen, F. Colizzi, S. De, M. De La Pierre, D. Donadio, V. Drobot, B. Ensing, A.L. Ferguson, M. Filizola, J.S. Fraser, H. Fu, P. Gasparotto, F. L. Gervasio, F. Giberti, A. Gil-Ley, T. Giorgino, G.T. Heller, G.M. Hocky, M. Iannuzzi, M. Invernizzi, K.E. Jelfs, A. Jussupow, E. Kirilin, A. Laio, V. Limongelli, K. Lindorff-Larsen, T. Löhr, F. Marinelli, L. Martin-Samos, M. Masetti, R. Meyer, A. Michaelides, C. Molteni, T. Morishita, M. Nava, C. Paissoni, E. Papaleo, M. Parrinello, J. Pfaendtner, P. Piaggi, G. Piccini, A. Pietropaolo, F. Pietrucci, S. Pipolo, D. Provasi, D. Quigley, P. Raiteri, S. Raniolo, J. Rydzewski, M. Salvalaglio, G.C. Sosso, V. Spiwok, J. Šponer, D.W.H. Swenson, P. Tiwary, O. Valsson, M. Vendruscolo, G.A. Voth, A. White, The, P. c. promoting transparency and reproducibility in enhanced molecular simulations, Nat. Methods 16 (2019) 670–673.

[43] G.A. Tribello, M. Bonomi, D. Branduardi, C. Camilloni, G. Bussi, PLUMED 2: new feathers for an old bird, Comput. Phys. Commun. 185 (2014) 604–613.

[44] M. Bonomi, D. Branduardi, G. Bussi, C. Camilloni, D. Provasi, P. Raiteri, D. Donadio, F. Marinelli, F. Pietrucci, R.A. Broglia, M. Parrinello, PLUMED: a portable plugin for free-energy calculations with molecular dynamics, Comput. Phys. Commun. 180 (2009) 1961–1972.

[45] L.B. Wright, J.P. Palafox-Hernandez, P.M. Rodger, S. Corni, T.R. Walsh, Facet selectivity in gold binding peptides: exploiting interfacial water structure, Chem. Sci. 6 (2015) 5204–5214.
[46] M.A. Abdelhamid, K. Motomura, T. Ikeda, T. Ishida, R. Hirota, A. Kuroda, Affinity purification of recombinant proteins using a novel silica-binding peptide as a fusion tag, Appl. Microbiol. Biotechnol. 98 (2014) 5677–5684.
[47] J. van den Boom, A. Hensel, F. Trusch, A. Matena, S. Siemer, D. Guel, D. Docter, A. Höing, P. Bayer, R.H. Stauber, S.K. Knauer, The other side of the corona: nanoparticles inhibit the protease taspase1 in a size-dependent manner, Nanoscale 12 (2020) 19093–19103.
[48] S.P. Schwaminger, S.A. Blank-Shim, I. Scheifele, P. Fraga-García, S. Berensmeier, Peptide binding to metal oxide nanoparticles, Faraday Discuss. 204 (2017) 233–250.
[49] J. Sampath, J. Pfaendtner, Amphiphilic peptide binding on crystalline vs. amorphous silica from molecular dynamics simulations, Mol. Phys. 117 (2019) 3642–3650.